# AERODYNAMICS OF BLUFF BODY CLOSE TO A MOVING GROUND

**Alex Mendonça Bimbato, alexbimbato@unifei.edu.br**
**Luiz Antonio Alcântara Pereira, luizantp@unifei.edu.br**
Institute of Mechanical Engineering, Federal University of Itajubá, CP 50, Av. BPS 1303, CEP 37500-903, Itajubá, Minas Gerais, Brazil.

**Miguel Hiroo Hirata, hirata@fat.uerj.br**
State University of Rio de Janeiro, FAT-UERJ, Resende, Rio de Janeiro, Brazil.

***Abstract.*** *This numerical study is related to the determination of aerodynamic loads of a circular cylinder in close proximity to a flat surface which travels at a uniform speed; the surface speed is the same as the velocity of the oncoming freestream. The main practical motivation comes from the automotive industry where a moving ground simulation is essential. A numerical model of a moving ground is represented by distributing source panels. For the moving conditions of each panel, the new coordinates of each panel are given at each time, and the one cycle of motion is produced by a number of steps of instantaneous ground configuration. The distance between the body and the moving ground, i.e., the gap-ratio ($h/d$) varies from $h/d = 0.05$ to $h/d = 0.60$ and the Reynolds number is fixed as higher value of 100,000. The numerical results from a two-dimensional circular cylinder in moving ground are compared with experimental results available in the literature and show that the drag coefficient decreases as the body comes close to the ground; besides that, when the gap ratio is too low there is a tendency of cessation of the vortex shedding by the separation points of the circular cylinder.*

***Keywords****: Ground Effect, Moving Ground, Blockage Effect; Aerodynamic Loads; Lagrangian Description.*

## 1. INTRODUCTION

The phenomenon of vortex shedding from a bluff body has been the object of numerous experimental and numerical studies due to the fundamental mechanisms that this flow exhibits and its numerous industrial applications. Only to quote an example, the alternate shedding of vortices in the near wake leads to large fluctuating pressure forces in a direction transverse to the flow and may cause structural vibrations, acoustic noise or resonance.

When a bluff body moves in close proximity to the ground, the ground will have an influence on the flow close to the body. When the fluid on the body separates and a large wake region develops, the separated flow also changes due to the ground effect. A typical example is the flow around a motor car; in this case the road is the ground. The calculation of such flows is very complex because of the large separated regions and the additional ground effect.

The relative motion between body and ground is usually neglected in experimental investigations; Roshko *et al*. (1975), Bearman and Zdravkovich (1978), Angrilli *et al*. (1982), and Price *et al*. (2002) studied the fundamental effects of the ratio of the gap between the cylinder and the ground, i.e., the gap ratio defined by $h/d$ ($d$ is the cylinder diameter), but all of them did not consider the relative motion between the body and the ground. Roshko *et al*. (1975) studied the time-averaged drag and lift coefficients, $C_D$ and $C_L$, for a circular cylinder placed near a fixed wall at $Re = 2.0\times10^4$ and showed that the $C_D$ decreased and $C_L$ increased as the cylinder came close to the wall. Zdravkovich (1985) observed, in his force measurements performed at $4.8\times10^4 < Re < 3.0\times10^5$, that the rapid decrease in drag occurred as the gap was reduced to less than the thickness of the boundary layer developed from the ground, $\delta$, and concluded that the variation of $C_D$ was dominated by $h/\delta$ rather than by the conventional gap ratio $h/d$.

Zdravkovich (2003) reported the drag behavior for a cylinder placed near a moving ground running at the same speed as the freestream. The Reynolds number was kept high ($Re = 2.5\times10^5$) and in the circumstances described above, there was practically no boundary layer on the ground. In contrast to the results obtained by Roshko *et al*. (1975), the decrease in drag due to the decrease in $h/d$ did not occur in his measurements. It was not clear, however, whether this was attributed to the non-existence of the wall boundary layer or the higher Reynolds number, or any other influencing factors.

Nishino (2007) studied the aerodynamic behavior of a circular cylinder placed near a moving belt in a wind tunnel. The moving belt velocity was the same as the oncoming flow and he turned back that there was practically no boundary layer developed on the ground. In his study the vortex shedding from a circular cylinder was investigated by visualizing air flows around it at Reynolds numbers of $4.0\times10^4 - 1.0\times10^5$. The three dimensional effects was taking into account by the use of end plates on the cylinder edges; for the cylinder with end-plates, on which the oil flow patterns were observed to be essentially two-dimensional, Nishino (2007) classified the flow into three regimes: large-gap

($h/d > 0.5$), intermediate-gap ($0.35 < h/d < 0.5$), and small-gap ($h/d < 0.35$) regimes. In the large-gap regime, large-scale, kármán-type vortices were generated just behind the cylinder, resulting in higher values of $C_D$ around 1.3. In contrast, in the small-gap regime, the large-scale vortex shedding totally ceased and instead a dead-fluid zone was created, bounded by two nearly parallel shear layers each producing only small-scale vortices in the near wake region. No substantial effect of $h/d$ was observed in this regime: $C_D$ was almost constant at a lower value of about 0.95. In the intermediate-gap regime, the kármán-type vortex shedding was found to be intermittent, i.e., typical instantaneous wake patterns of both the large and small-gap regimes were intermittently observed, and $C_D$ rapidly decreased as $h/d$ decreased from 0.5 to 0.35.

Bimbato *et al*. (2009) used the conclusions reported by Zdravkovich (2003) and Nishino (2007), i.e., that there was practically no boundary layer on the ground when the moving ground runs at the same speed as the freestream, and used the Vortex Method to simulate numerically the motion of a plane surface by the suppression of its boundary layer. In that situation, the ground remained rest and its motion was represented only by the boundary layer suppression. The aerodynamic loads obtained numerically were compared with the experimental results gained by Nishino (2007) for the large and intermediate-gap regimes.

The present work deals with the Vortex Method with a turbulence modeling to study the two-dimensional, incompressible unsteady flow of a Newtonian fluid with constant properties around a circular cylinder placed near a moving ground; in contrast of Bimbato *et al*. (2009), in this paper the plane surface have a motion (physically) with the same speed as the oncoming flow. In this more realistic configuration in which the plane surface moves like a moving belt of a wind tunnel, the aerodynamic loads are investigated to gap-ratios that cover the three flow regimes identified by Nishino (2007). Besides that, it is shown the mechanisms of vortex structures detachment from the separation points of the body.

The Vortex Method using Large Eddy Simulation (Alcântara Pereira *et al*., 2002) is chosen because it offers a number of advantages over the traditional Eulerian schemes for the analysis of the external flow that develops in a large domain; the main reasons are [Leonard (1980), Sarpkaya (1989), Lewis (1999), Kamemoto (2004), and Stock (2007)]: (i) the absence of a mesh avoids stability problems of explicit schemes and mesh refinement problems; (ii) the lagrangian description eliminates the need to explicitly treat convective derivatives; (iii) all the calculation is restricted to the rotational flow regions and no explicit choice of the outer boundaries is needed a priori; (iv) no boundary condition is required at the downstream end of the fluid domain.

## 2. MATHEMATICAL FORMULATION

Figure 1 presents schematically the two-dimensional unsteady and incompressible flow of a Newtonian fluid with constant properties which drain around a circular cylinder placed near a plane surface, or ground. The ground has the same speed as the oncoming flow. One can define: the incident flow ($U$); the semi-infinity fluid domain ($\Omega = S_1 \cup S_2 \cup S_3$), where $S_1$ is the body surface, $S_2$ is the plane surface and $S_3$ is the surface defined far from the body.

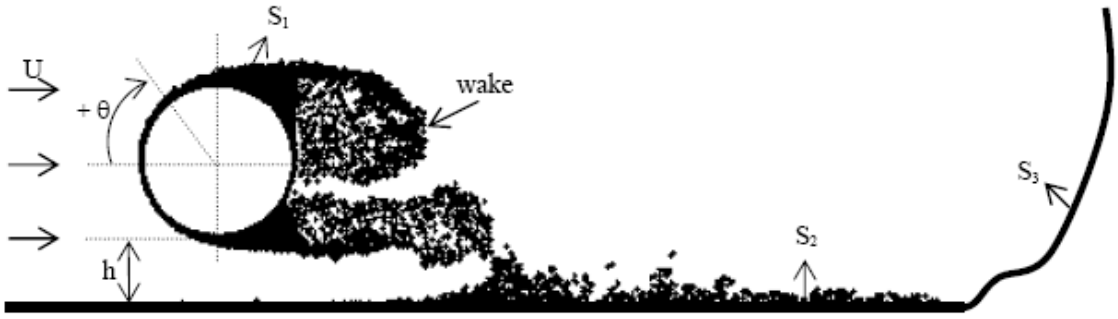


Figure 1. Definition of the fluid region

The problem is governed by the continuity and the Navier-Stokes equations, which can be written in the form:

$$\frac{\partial \overline{u_i}}{\partial x_i} = 0, \tag{1}$$

where $\overline{u}$ is the velocity field filtered or the macro-scale field (Smagorinsky, 1963),

$$\frac{\partial \overline{u_i}}{\partial t} + \frac{\partial}{\partial x_j}\left(\overline{u_i}\,\overline{u_j}\right) = -\frac{1}{\rho}\frac{\partial \overline{p}}{\partial x_i} + 2\frac{\partial}{\partial x_j}\left[\left(\nu + \nu_t\right)\overline{S_{ij}}\right], \tag{2}$$

where $\overline{p}$ is the pressure field filtered, $\rho$ is the density, $\nu$ is the molecular viscosity coefficient, $\nu_t$ is the eddy viscosity coefficient, and the deformation tensor of the filtered field is defined as:

$$\overline{S_{ij}} = \frac{1}{2}\left(\frac{\partial \overline{u_i}}{\partial x_j} + \frac{\partial \overline{u_j}}{\partial x_i}\right). \tag{3}$$

When using lagrangian vortex method, the model proposed by Smagorinsky (1963) is inconvenient by the use of deformation rate (derivatives).

As an alternative, Métais and Lesieur (1992) considered that the small scales may not be too far from isotropic and proposed to use the local kinetic-energy spectrum $E_{(K_c)}$ at the cut-off wave number ($K_c$) to define the eddy viscosity, $\nu_t$.

Using a relation given by Batchelor (1953), Lesieur and Métais (1996) proposed to calculate the local spectrum at $K_c$ with a second-order velocity structure function $\overline{F_2}$ of the filtered field:

$$\overline{F_2}\left(\boldsymbol{x}, \Delta, t\right) = \left\| \overline{\boldsymbol{u}}\left(\boldsymbol{x}, t\right) - \overline{\boldsymbol{u}}\left(\boldsymbol{x} + \boldsymbol{r}, t\right) \right\|^2_{\|\boldsymbol{r}\| = \Delta}. \tag{4}$$

From the Kolmogorov spectrum the eddy viscosity can be written as a function of $\overline{F_2}$:

$$\nu_t\left(x, \Delta\right) = 0.105\, C_K^{-\frac{3}{2}}\, \Delta \sqrt{\overline{F_2}\left(\boldsymbol{x}, \Delta, t\right)}, \tag{5}$$

where $C_k = 1.4$ is the Kolmogorov constant.

In Eq. (4) is important to note that the "average operator" is applied in the velocities $\boldsymbol{u}\left(\boldsymbol{x} + \boldsymbol{r}, t\right)$ calculated under the surface of a sphere with center in $\boldsymbol{x}$ and radius $|\boldsymbol{r}|$.

The great advantage of the formulation presented above is the use of the concept of velocity fluctuation (differences) to be combined with Lagrangian Vortex Method.

Therefore, the strategy is to study the vorticity dynamic using the continuity equation, Eq. (1), and the Navier-Stokes equations, Eq. (2), to simulate the phenomena that occur in the macro-scales with the lagrangian Vortex Method. The phenomena that occur in the micro-scales should be take into account through the eddy viscosity coefficient, Eq. (5); this coefficient ($\nu_t$) is modeled with the second-order velocity structure function $\overline{F_2}$ of the filtered field; see Eq. (4).

It is necessary to impose the boundary conditions. The impenetrability condition demands that the normal velocity component of the fluid particle ($u_n$) should be equal to the normal velocities components of the surfaces $S_1$ and $S_2$ ($v_n$):

$$u_n - v_n = 0 \text{, on } S_1 \text{ and } S_2, \tag{6}$$

The no-slip condition demands that the tangential velocity component of the fluid particle ($u_\tau$) should be equal to the tangential velocity component of the surfaces $S_1$ and $S_2$ ($v_\tau$):

$$u_\tau - v_\tau = 0 \text{, on } S_1 \text{ and } S_2. \tag{7}$$

The last boundary condition to be imposed is that, far away, the perturbation caused by the solid boundaries fades as:

$$|\boldsymbol{u}| \to U \text{, on } S_3. \tag{8}$$

## 3. SOLUTION METHOD: THE VORTEX METHOD

The dynamics of the lift motion is studied by taking the curl of the Eq. (2), obtaining the new 2-D vorticity equation (Alcântara Pereira *et al*., 2002):

$$\frac{\partial \omega}{\partial t} + (\boldsymbol{u} \cdot \nabla)\omega = \frac{1}{Re_c}\nabla^2 \omega \,, \tag{9}$$

where the bars that identified the filtered field were omitted and the modified Reynolds number is defined in Eq. (13).

Chorin (1973) proposed the "Viscous Splitting Algorithm" to simplify the numerical implementation of the Vortex Method; with this algorithm, in the same time increment, the convective effects are solved independently of the viscous diffusion effects. In this way, the convective equation takes the Lagrangian form:

$$\frac{D\omega}{Dt} = 0 \tag{10}$$

On the other hand, the diffusive equation is given by:

$$\frac{\partial \omega}{\partial t} = \frac{1}{Re_c}\nabla^2 \omega \tag{11}$$

It is obvious from the equation above that the viscosity effects are taking into account in the diffusive process.

Alcântara Pereira *et al.* (2002) make two adaptations necessary to implement the second-order velocity structure function to the 2-D Lagrangian Vortex Method; see Eq. (4): (i) the points where the velocities must be calculated are placed inside a circular crown defined by $r_i = 0.1\sigma_0$ and $r_e = 2.0\sigma_0$, where $r_i$ and $r_e$ are the internal and external radius of the circular crown, respectively, and $\sigma_0$ is the Lamb vortex core of the vortex under analysis (see Eq. (14)); (ii) to compute the second-order velocity structure function, the points where the velocities are calculated are the same as the positions of the vortices which are near the vortex under analysis and finally:

$$\overline{F_2} = \frac{1}{NV}\sum_{i=1}^{NV} \left\| \boldsymbol{u}_t(\boldsymbol{x}) - \boldsymbol{u}_t(\boldsymbol{x} + \boldsymbol{r}_i) \right\|_i^2 \left( \frac{\sigma_0}{\boldsymbol{r}_i} \right)^{2/3} , \tag{12}$$

where $\boldsymbol{u}_t$ is the total velocity in the point, $NV$ indicates the number of vortices inside the circular crown and $r_i$ is the distance between the vortex under analysis and the vortices inside the circular crown.

In the sequence, the eddy viscosity coefficient is calculated making $\Delta = \sigma_0$ in Eq. (5). After this, the modified Reynolds number can be defined as:

$$Re_c = \frac{U\,d}{\nu + \nu_t} , \tag{13}$$

where $d$ is the cylinder diameter and the dimensionless time is $d/U$. The Lamb vortex core is calculated as (Alcântara Pereira *et al.*, 2002):

$$\sigma_{0_{\nu_t}} = 4.48364\sqrt{\frac{\Delta t}{Re}\left(1 + \frac{\nu_t}{\nu}\right)} , \tag{14}$$

where $\Delta t$ is the time increment of the numerical simulation.

To solve the convective problem is necessary to determine the velocity field which is composed by three contributions: the contribution due to the incident flow, $\boldsymbol{ui}(\boldsymbol{x},t)$, solid boundaries, $\boldsymbol{ub}(\boldsymbol{x},t)$, and the vortex-vortex interaction, $\boldsymbol{uv}(\boldsymbol{x},t)$. Thus:

$$\boldsymbol{u_i}(\boldsymbol{x},t) = \boldsymbol{ui}(\boldsymbol{x},t) + \boldsymbol{ub_i}(\boldsymbol{x},t) + \boldsymbol{uv_i}(\boldsymbol{x},t), \; i = 1, Z \tag{15}$$

where $Z$ is the total number of Lamb discrete vortices in the wake.

The contribution of the incident flow is given by:

$$ui_1 = 1 \text{ and } ui_2 = 0 . \tag{16}$$

The contribution of the solid boundaries is given by the source Panel's Method (Katz and Plotkin, 1991), so:

$$ub_i\left(x_j,t\right) = \sum_{k=1}^{NP} \sigma_k c_{jk}^i \left[x_j\left(t\right) - x_k\right],\ i = 1,2 \text{ and } j = 1,Z , \tag{17}$$

where $NP$ is the number of flat panels that represents the solid boundaries, $\sigma_k = const$ is the density of sources per unit length and $c_{jk}^i\left(x_j\left(t\right) - x_k\right)$ is the $i$ component of the velocity induced at discrete vortex $j$ by $k$ panel.

Finally, the contribution of the vortex cloud is given by:

$$uv_i\left(x_j,t\right) = \sum_{k=1}^{Z} \Gamma_k c_{jk}^i \left(x_j\left(t\right) - x_k\left(t\right)\right),\ i = 1,2 \text{ and } j = 1,Z , \tag{18}$$

where $\Gamma_k$ is the intensity of the $k$ vortex and $c_{jk}^i\left(x_j\left(t\right) - x_k\right)$ is the $i$ component of the induced velocity in a discrete vortex $j$ by a $k$ discrete vortex.

With the velocity field, the convection is calculated by a first order Euler scheme:

$$\boldsymbol{x_i}\left(t + \Delta t\right) = \boldsymbol{x_i}\left(t\right) + \boldsymbol{u_i}\left(\boldsymbol{x_i}\left(t\right), t\right)\Delta t ,\ i = 1,Z . \tag{19}$$

The diffusion equation, Eq. (11), is solved by the random walk scheme (Lewis, 1999), which consists in add a random displacement to Eq. (19):

$$\zeta_i\left(t\right) = \sqrt{\frac{4\,\Delta t}{Re_c} ln\left(\frac{1}{P}\right)}\left[cos 2\pi Q + sen\, 2\pi Q\right], \tag{20}$$

where $P$ and $Q$ are random numbers with $0 < P < 1$ and $0 < Q < 1$.

Once, with the vorticity field the pressure calculation starts with the Bernoulli function, defined by Uhlman (1992) as:

$$\overline{Y} = p + \frac{u^2}{2},\ u = \left|\boldsymbol{u}\right| . \tag{21}$$

Kamemoto (1993) used the same function and starting from the Navier-Stokes equations was able to write a Poisson equation for the pressure. This equation was solved using a finite difference scheme. Here the same Poisson equation was derived and its solution was obtained through the following integral formulation (Shintani and Akamatsu, 1994):

$$H\overline{Y_i} - \int_S \overline{Y} \nabla \Xi_i \cdot \boldsymbol{e_n}\, dS = \iint_\Omega \nabla \Xi_i \cdot \left(\boldsymbol{u} \times \boldsymbol{\omega}\right) d\Omega - \frac{1}{Re} \int_S \left(\nabla \Xi_i \times \boldsymbol{\omega}\right) \cdot \boldsymbol{e_n}\, dS , \tag{22}$$

where $H = 1.0$ in the fluid domain, $H = 0.5$ on the boundaries, $\Xi$ is a fundamental solution of the Laplace equation and $\boldsymbol{e_n}$ is the unit vector normal to the solid surfaces.

The drag and lift coefficients are expressed by:

$$C_D = -\sum_{k=1}^{NP} C_p \Delta S_k sen\beta_k , \tag{23}$$

$$C_L = -\sum_{k=1}^{NP} C_p \Delta S_k cos\beta_k , \tag{24}$$

where $\Delta S_k$ is the length and $\beta_k$ is the angle and both of the $k$ panel.

## 4. RESULTS AND DISCUSSION

### 4.1. Flow around an isolated circular cylinder

The analysis of the aerodynamic behavior of an isolated circular cylinder was made in order to obtain the parameters that influence the numerical method and the turbulence modeling; the isolated circular cylinder is a classical problem in fluid mechanics so it is a great starting point to validate the code. To obtain the result shown is Tab. 1 the surface of circular cylinder was represented by $mb = 300$ sources flat panels with constant distribution in order to ensure the impenetrability condition (Eq. (6)); the no slip condition (Eq. (7)) was ensured by the generation of discrete Lamb vortices with core $\sigma_0 = 0.001$, which are positioned in a perpendicular distant $eps = 0.001$ normal from the control point of each panel. The Reynolds number studied was $1.0 \times 10^5$.

Table 1. Mean values of drag and lift coefficients and Strouhal number for an isolated circular cylinder

| $Re = 1.0 \times 10^5$ | $\overline{C}_D$ | $\overline{C}_L$ | $\overline{St}$ |
|---|---|---|---|
| Blevins (1984) | 1.20 | - | 0.19 |
| Present Simulation | 1.30 | 0.02 | 0.21 |

Table 1 show that the drag coefficient is inside the uncertainty band of 10% specified by Blevins (1984). The lift coefficient is not zero due to numerical errors inherent of any numerical method. The Strouhal number is defined as:

$$St = \frac{f\,d}{U}, \tag{25}$$

where $f$ is the frequency of detachment of the vortex structures from the separation points of the circular cylinder. In the next item the mechanism of these structures formation will be discussed.

With the results gained by the numerical code in the simulation of the flow around an isolated circular cylinder one can consider the code able to simulate the ground effect phenomenon. In the simulations made in order to study the ground effect the numerical parameters used in the isolated circular cylinder case were maintained and the moving ground surface was represented by $mg = 200$ sources flat panels. More details about the flow around an isolated circular cylinder in order to validate de numerical code can be seen in Bimbato (2008).

### 4.2. Circular cylinder in ground effect

In the present study the authors impose a motion on the plane surface with the same velocity of the oncoming flow ($mov = U = 1$). The purpose is to study the influence of the distance between the body and the ground on the aerodynamic behavior of a circular cylinder and compare the numerical results with the experimental ones obtained by Nishino (2007).

In his experimental study, Nishino (2007) shows the influence of the tip effect on the aerodynamic behavior of the body. In order to study the approximately two dimensional flow, Nishino (2007) fixed end-plates on the cylinder extremities; this configuration is referred as $y/d = 0.0$ and $y/d = 0.4$ on Tab. 2, where the greater value of the relation $y/d$ represents the configuration in which the flow is closer to a 2-D configuration. So, the comparison between the numerical results of the present work with the experimental ones obtained by Nishino (2007) with the ratio $y/d = 0.4$ is a great opportunity to show the Vortex Method competence to reproduce experimental work features. The comparison for the drag coefficient is given in Tab. 2.

It can be notice that for the configuration closer to a two dimensional flow studied by Nishino (2007), $y/d = 0.4$, the numerical results are in good agreement with the experimental ones, showing a difference of approximately 8%, which is acceptable for numerical simulations.

Table 2. Comparison between the numerical results obtained with the Vortex Method with LES scheme with the ones obtained by Nishino (2007) for the drag coefficient

| $h/d$ | Nishino (2007) - $y/d = 0.0$ | Nishino (2007) - $y/d = 0.4$ | Present Simulation |
|---|---|---|---|
| 0.05 | 0.941 | - | 1.263 |
| 0.15 | 0.957 | - | 1.188 |
| 0.40 | 1.145 | - | 1.370 |
| 0.45 | 1.242 | 1.311 | 1.418 |
| 0.50 | 1.282 | 1.323 | 1.405 |
| 0.60 | 1.302 | 1.373 | 1.435 |

It can be seen that even for the case of $y/d = 0.0$ the Vortex Method with a Large Eddy Simulation is able to anticipate the drag drop as the body come close to the ground. Figure 2 shows the evolution of the aerodynamic loads for some gap-ratios, $h/d$, which are inside of the three gap regimes identified by Nishino (2007): (i) large gap-ratios ($h/d > 0.5$) – Fig. 2a; (ii) intermediate gap-ratios ($0.35 < h/d < 0.50$) – Fig. 2b; (iii) small gap-ratios ($h/d < 0.35$) – Fig. 2c and Fig. 2d.

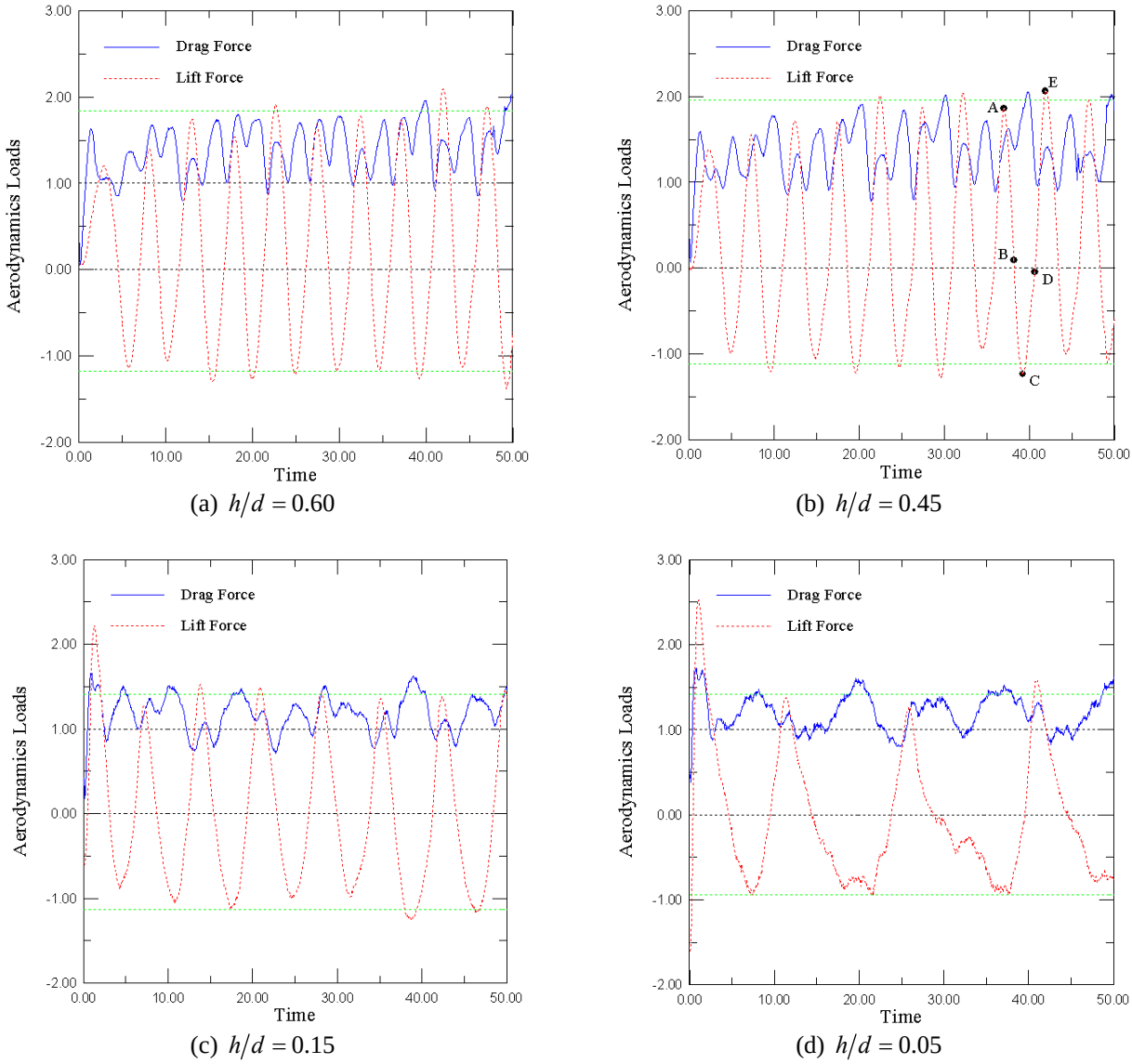


(a) $h/d = 0.60$ (b) $h/d = 0.45$

(c) $h/d = 0.15$ (d) $h/d = 0.05$

Figure 2 – Evolution of the aerodynamic loads for a circular cylinder in ground effect

According to Tab.2 the configuration closer to a two dimensional flow ($y/d = 0.4$) has $h/d = 0.45$ as the smaller gap-ratio. So this gap-ratio will be used to explain the mechanism of vortex formation from the circular cylinder in ground effect with numerical simulations using the Vortex Method.

To explain this mechanism considers Fig. 2b, which has some points (A, B, C, D and E) that represent important moments where interesting flow features happen. Figure 3 presents the pressure distribution on these important moments.

At the instant represented by point A it can be seen that there is a low pressure distribution in the upper surface of the cylinder. However, at the instant represented by point C there is a low pressure distribution in the lower surface of the cylinder (see Fig. 3). These instants correspond to the birth of a clockwise vortex structure on the upper surface of the cylinder (point A) and a counter clockwise vortex structure on the lower surface of the circular cylinder (point C) as can be seen in Fig. 4a and Fig. 4c.

The lower pressure distributions described above are the responsible for the maximum lift coefficient at points A and E and for the minimum lift coefficients at point C; see Fig. 2b.

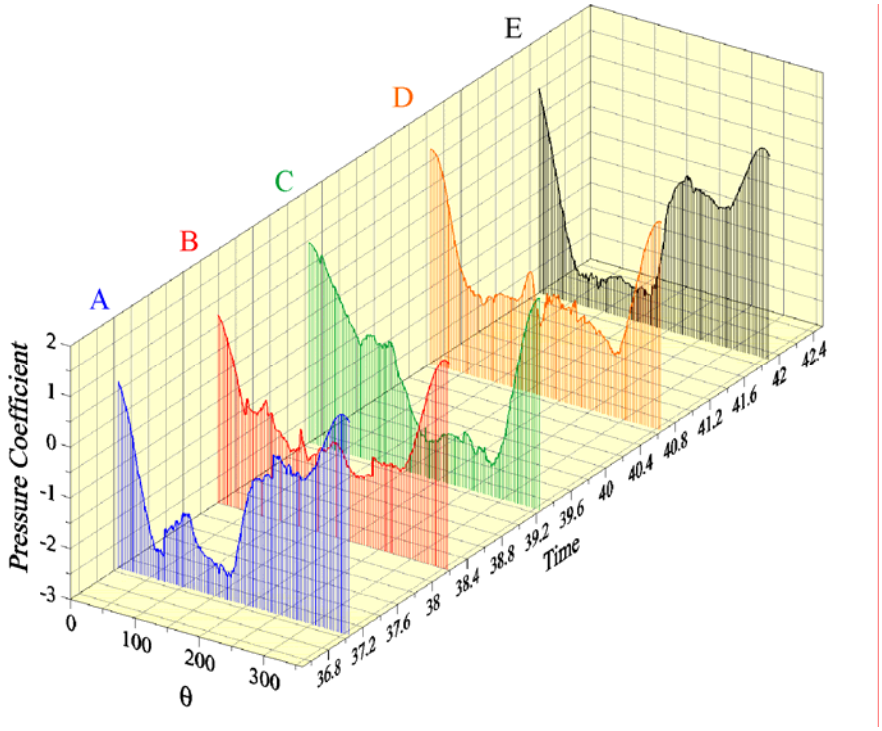


Figure 3. Instantaneous pressure distribution around the circular cylinder in ground effect ( $h/d = 0.45$ )

Simultaneously the drag coefficient at the instant represent by point $A \equiv E$ are increasing due to the growth of the counter clockwise structure birthed at an instant represented by point C which is getting energy attracting the opposite shear structure and reaches a critical level of energy (maximum drag coefficient) and starts to be incorporated by the viscous wake (see Fig. 4a), which causes a decrease on the drag coefficient.

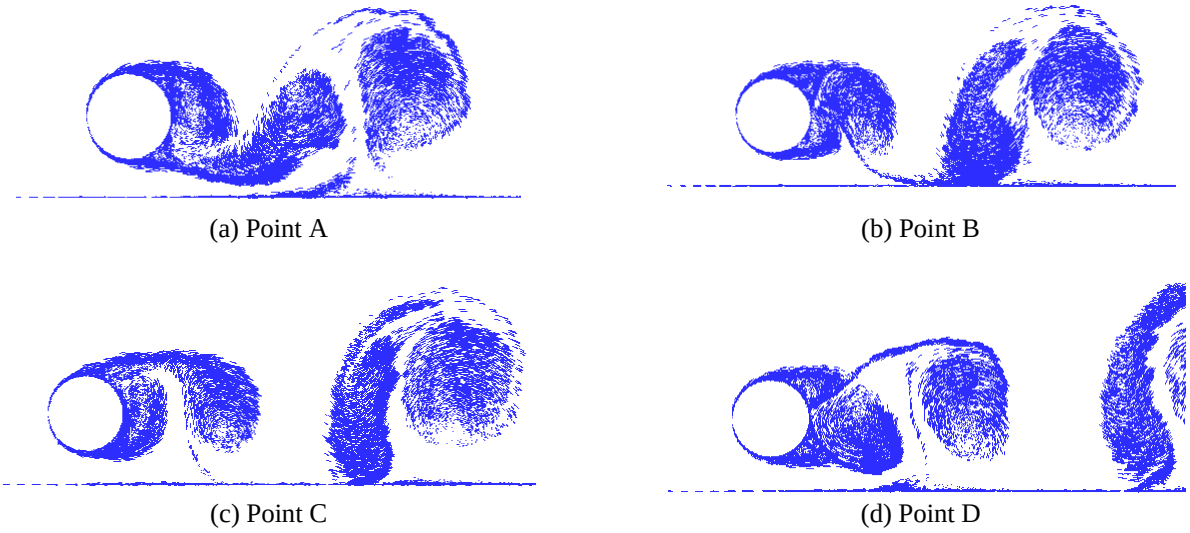

(a) Point A

(b) Point B

(c) Point C

(d) Point D

Figure 4. Details of the vortex structure detachment from a circular cylinder in ground effect ( $h/d = 0.45$ )

This mechanism is dynamic in a manner that at the instant represented by point C the drag coefficient is increasing too, but due to the clockwise structure that birthed at an instant represented by point A, which starts to grow getting energy from the opposite shear layer (Fig. 4b); when the clockwise structure reaches a critical level of energy (maximum $C_D$ ), it starts to be incorporated by the viscous wake (Fig. 4c) and the process repeats all over again, like described by Gerrard (1966).

However there is an interesting feature in Fig. 2b: the drag coefficient curve presents peaks sometimes bigger, sometimes smaller. This occurs due to the blockage effect imposed by the moving ground; the vortex structure that was born in the upper surface of the body (point A) has total freedom to grow until to be incorporated by the viscous wake

(point C), which results in a bigger peak of the drag coefficient at this instant (point C). On the other hand, the growth of the structure that was born on the lower surface of the body (point C) is limited by the moving ground when this vortex structure is been incorporated by the viscous wake (point $A \equiv E$), which causes a smaller peak on the drag coefficient at this instants (point $E \equiv A$).

The drag drop verified as the cylinder come close to the ground (see Tab. 2) occurs due to the flow configuration; when the moving ground runs at the same speed as the oncoming flow, in a essentially three dimensional flow configuration the drag coefficient increases as the cylinder come close to the ground (Nishino, 2007). Thus it can be notice that the flow configuration (3D or 2D) is another mechanism that governs the ground effect phenomenon. However, the numerical simulations made here are two dimensional in a manner that is impossible to discuss this mechanism in this study.

In order to investigate the smaller gap regime ($h/d < 0.35$) (Nishino, 2007), the authors show in Tab.3 the Strouhal number for some gap ratios ($h/d$).

Table 3. Mean Strouhal number for some gap ratios, $h/d$

| $h/d$ | $\overline{St}$ |
|---|---|
| 0.05 | 0.07 |
| 0.15 | 0.14 |
| 0.40 | 0.20 |
| 0.45 | 0.20 |
| 0.50 | 0.20 |
| 0.60 | 0.20 |

Nishino (2007) reveals that for $h/d < 0.35$ the formation of bigger vortex structures is ceased. This seems to be true when ones analyses Tab. 3 with the aerodynamic loads showed in Fig. 2c and Fig. 2d. Besides that, the wakes in Fig. 5 show a tendency of an interruption of this structures formation. However the authors advise that is necessary to improve the discrete vortex generation process when the body is too close to the ground to confirm this tendency.

(a) $h/d = 0.15$ (b) $h/d = 0.05$

Figure 5. Position of the vortices in the wake at the end of the simulation of a circular cylinder in ground effect

The simulations presented in this study have duration of 628h (approximately 27 days) in a Quad Core Intel processor.

## 5. CONCLUSIONS

The ground effect phenomenon is far from being fully understood, in despite of many investigations made by the scientific community. The difficulty is due to the many influential factors that govern the phenomenon, such as the blockage effect imposed by the moving ground, the wake interference effect, where the viscous wake interacts with the boundary layer developed from the ground, the three dimensional effects and the gap-ratio, $h/d$.

Although the numerical simulations are two dimensional they contributed in order to understand some factors that govern the phenomenon, like the blockage effect that changes the drag coefficient curve, causing peaks sometimes bigger, sometimes smaller and the gap-ratio which causes the drag drop in 2-D flows.

Finally, it is important to mention that the simulations used to obtain the numerical results presented in this paper are more realistic since they work with moving boundary problems, which changes the ground geometry in each time step; however it is important to use algorithms that make the code faster, like a parallel code, to make possible more refined simulations to work together with experimental analysis in order to understand better the physics involved on the ground effect phenomenon.

## 6. ACKNOWLEDGEMENTS

This research was supported by the CNPq (Brazilian Research Agency) Proc. 470420/2008-1, FAPEMIG (Research Foundation of the State of Minas Gerais) Proc. TEC APQ-01074-08 and FAPERJ (Research Foundation of the State of Rio de Janeiro) Proc. E-26/112/013/08.

## 7. REFERENCES

Alcântara Pereira, L. A., Ricci, J. E. R., Hirata, M. H., Silveira Neto, A., 2002, "Simulation of the Vortex-Shedding Flow about a Circular Cylinder with Turbulence Modeling", CFD Journal, Vol. 11, No. 3, october, pp. 315-322.

Angrilli, F., Bergamaschi, S. and Cossalter, V., 1982, "Investigation of Wall Induced Modifications to Vortex Shedding from a Circular Cylinder", Transactions of the ASME: Journal of Fluids Engineering, Vol. 104, pp. 518-522.

Batchelor, G. K., 1953, "The Theory of Homogeneous Turbulence", Cambridge University Press.

Bearman, P. W. and Zdravkovich, M. M., 1978, "Flow around a Circular Cylinder near a Plane Boundary", Journal of Fluid Mechanics, Vol. 89, pp. 33-47.

Bimbato, A. M., 2008, Analysis of Moving Ground Effects on the Aerodynamic Loads of a Body, M.Sc. Dissertation, IEM/UNIFEI (in Portuguese).

Bimbato, A. M., Alcântara Pereira, L. A., Hirata, M. H., 2009, "Simulation of Viscous Flow around a Circular Cylinder near a Moving Ground", J. of the Braz. Soc. of Mech. Sci. & Eng., Vol. XXXI, No. 3, pp. 243-252.

Blevins, R. D., 1984, Applied Fluid Dynamics Handbook, Van Nostrand Reinhold, Co.

Chorin, A. J., 1973, "Numerical Study of Slightly Viscous Flow", Journal of Fluid Mechanics, Vol. 57, pp. 785-796.

Gerrard, J. H., 1966, "The Mechanics of the Formation Region of Vortices behind Bluff Bodies", J. Fluid Mech., 25: 401-413.

Kamemoto, K., 1993, "Procedure to Estimate Unstead Pressure Distribution for Vortex Method" (In Japanese), Trans. Jpn. Soc. Mech. Eng., Vol. 59, No. 568 B, pp. 3708-3713.

Kamemoto, K., 2004, "On Contribution of Advanced Vortex Element Methods Toward Virtual Reality of Unsteady Vortical Flows in the New Generation of CFD", Proceedings of the 10th Brazilian Congress of Thermal Sciences and Engineering-ENCIT 2004, Rio de Janeiro, Brazil, Nov. 29 - Dec. 03, Invited Lecture-CIT04-IL04.

Katz, J. and Plotkin, A., 1991, "Low Speed Aerodynamics: From Wing Theory to Panel Methods", McGraw Hill, Inc.

Leonard, A., 1980, "Vortex Methods for Flow Simulation", J. Comput. Phys., Vol. 37, pp. 289-335.

Lesieur, M. and Métais, O., 1996, "New trends in large-eddy simulation of turbulence". A Review in Fluid Mechanics, Vol. 28, pp. 45-82.

Lewis, R. I., 1999, "Vortex Element Methods, the Most Natural Approach to Flow Simulation - A Review of Methodology with Applications", Proceedings of 1st Int. Conference on Vortex Methods, Kobe, Nov. 4-5, pp. 1-15.

Métais, O. and Lesieur, M., 1992, "Spectral Large-Eddy Simulations of Isotropic and Stably-Statified Turbulence", J. Fluid Mech., 239, pp. 157-194.

Nishino, T., 2007, Dynamics and Stability of Flow Past a Circular Cylinder in Ground Effect, Ph.D. Thesis, Faculty of Engineering, Science and Mathematics, University of Southampton, 145p.

Price, S. J., Summer, D., Smith, J. G., Leong, K. and Paidoussis, M. P., 2002, "Flow Vizualization around a Circular Cylinder near to a Plane Wall", Journal of Fluids and Structures, Vol. 16, pp. 175-191.

Roshko, A., Steinolfson, A. and Chattoorgoon, V., 1975, "Flow Forces on a Cylinder near a Wall or near another Cylinder", Proceedings of the 2nd U.S. National Conference on Wind Engineering Research, Fort Collins, Paper IV-15.

Sarpkaya, T., 1989, "Computational Methods with Vortices - The 1988 Freeman Scholar Lecture", Journal of Fluids Engineering, Vol. 111, pp. 5-52.

Shintani, M. and Akamatsu, T., 1994, "Investigation of Two Dimensional Discrete Vortex Method with Viscous Diffusion Model", Computational Fluid Dynamics Journal, Vol. 3, No. 2, pp. 237-254.

Smagorinsky, J., 1963, "General circulation experiments with the primitive equations", Mon. Weather Rev. 91,3,0099-164.

Stock, M. J., 2007, "Summary of Vortex Methods Literature (A lifting document rife with opinion)", April, 18: © 2002-2007 Mark J. Stock.

Uhlman, J. S., 1992, "An Integral Equation Formulation of the Equation of an Incompressible Fluid", Naval Undersea Warfare Center, T.R. 10-086.

Zdravkovich, M. M., 1985, "Forces on a Circular Cylinder near a Plane Wall", Applied Ocean Research, Vol. 7, pp. 197-201.

Zdravkovich, M. M., 2003, Flow around Circular Cylinders: Vol. 2: Applications, Oxford University Press, Oxford, UK.

## 8. RESPONSIBILITY NOTICE

The authors are the only responsible for the printed material included in this paper.